

Supporting information for

Projected increase in compound drought and hot days over global maize areas under global warming

Content

- 1. Calculation method**
- 2. Figures**
- 3. Tables**

1. Calculation method

1.1 SPI calculation method

For each wheat planting grid, the 1-month SPI are calculated for all months during 1950-2100. The calculation processes of SPI are as follows.

The probability density function (PDF) of the monthly precipitation series is fitted by Gamma function:

$$g(P) = \frac{1}{\beta^\alpha \Gamma(\alpha)} P^{\alpha-1} e^{-P/\beta} \quad (1)$$

$$\alpha = \frac{1}{4A} \left(1 + \sqrt{1 + \frac{4A}{3}}\right) \quad (2)$$

$$\beta = \frac{\bar{P}}{\alpha} \quad (3)$$

$$A = \ln(\bar{P}) - \frac{\sum \ln(P)}{n} \quad (4)$$

Where α and β are shape parameter and scale parameter that estimated by the maximum likelihood estimation method, P is monthly precipitation, n is the number of months. $\Gamma(\alpha)$ is given by:

$$\Gamma(\alpha) = \int_0^\infty k^{\alpha-1} e^{-k} dk \quad (5)$$

The cumulative distribution function (CDF) can be calculated by:

$$G(P) = \int_0^P g(P) dP = \frac{1}{\beta^\alpha \Gamma(\alpha)} \int_0^P P^{\alpha-1} e^{-P/\beta} dP \quad (6)$$

Since the Gamma function is undefined for $P=0$, thus $G(P)$ is adjusted as:

$$H(P) = q + (1 - q)G(P) \quad (7)$$

Where q is the probability of $P=0$.

Then the CDF can be transformed to the standard normal distribution function of t :

$$H(P) = \frac{1}{\sqrt{2\pi}} \int_{-\infty}^P e^{-\frac{t^2}{2}} dt \quad (8)$$

And SPI can be calculated from this normal distribution function:

$$\text{SPI} = \begin{cases} -\left(t - \frac{b_0 + b_1 t + b_2 t^2}{1 + c_1 t + c_2 t^2 + c_3 t^3}\right), t = \sqrt{\ln\left(\frac{1}{(H(P))^2}\right)}, \text{ when } 0 < H(P) \leq 0.5 \\ \left(t - \frac{b_0 + b_1 t + b_2 t^2}{1 + c_1 t + c_2 t^2 + c_3 t^3}\right), t = \sqrt{\ln\left(\frac{1}{(1.0 - H(P))^2}\right)}, \text{ when } 0.5 < H(P) \leq 1 \end{cases} \quad (9)$$

Where $b_0 = 2.515517$, $b_1 = 0.802853$, $b_2 = 0.010328$, $c_1 = 1.432788$, $c_2 = 0.189269$, $c_3 = 0.001308$.

1.2 SPEI calculation method

For each wheat planting grid, the 1-month SPEI are calculated for all months during 1950-2100. The calculation processes of SPEI are similar to SPI, the difference is that SPI is calculated based on monthly precipitation, while SPEI is calculated based on the difference between precipitation (P) and potential evapotranspiration (PET). The calculation processes of SPEI are as follows.

First, monthly PET is calculated based on Thornthwaite method [75]:

$$PET = 16K\left(\frac{10T}{I}\right)^m \quad (10)$$

$$I = \sum_{i=1}^{12} \left(\frac{T}{5}\right)^{1.514} \quad (11)$$

$$m = 6.75 \times 10^{-7} \times I^3 - 7.71 \times 10^{-5} \times I^2 + 1.79 \times 10^{-2} \times I + 0.492 \quad (12)$$

$$K = \left(\frac{N}{12}\right)\left(\frac{NDM}{30}\right) \quad (13)$$

where N is the maximum of sunlight hours, NDM is the number of days in a month. T is the mean monthly temperature ($^{\circ}\text{C}$), I is the annual thermal index, and m is given by a third-order polynomial of I .

Second, the monthly difference between precipitation and PET is calculated:

$$D_i = P_i - PET_i \quad (14)$$

Third, the probability density function (PDF) of the D_i series is fitted by three-parameters Log-logistic probability distribution function:

$$f(x) = \frac{\beta}{\alpha} \left(\frac{x-\gamma}{\alpha}\right)^{\beta-1} \left[1 + \left(\frac{x-\gamma}{\alpha}\right)^{\beta}\right]^{-2} \quad (15)$$

Where α , β and γ are scale, shape and origin parameters respectively. The cumulative distribution function of the D_i series is then given as:

$$F(x) = \left[1 + \left(\frac{\alpha}{x-\gamma}\right)^{\beta}\right]^{-1} \quad (16)$$

Forth, SPEI can be calculated from the normalization of $F(x)$:

$$P = 1 - F(x) \quad (17)$$

$$\text{SPEI} = \begin{cases} \omega - \frac{c_0 + c_1\omega + c_2\omega^2}{1 + d_1\omega + d_2\omega^2 + d_3\omega^3}, \omega = \sqrt{-2\ln(P)}, \text{ when } P \leq 0.5 \\ -(\omega - \frac{c_0 + c_1\omega + c_2\omega^2}{1 + d_1\omega + d_2\omega^2 + d_3\omega^3}), \omega = \sqrt{-2\ln(1 - P)}, \text{ when } P > 0.5 \end{cases} \quad (18)$$

Where $c_0 = 2.515517$, $c_1 = 0.802853$, $c_2 = 0.010328$, $d_1 = 1.432788$, $d_2 = 0.189269$, $d_3 = 0.001308$.

1.3 Mann-Kendall trend test

A combination of the Mann-Kendall (MK) trend test and the Theil-Sen approach (TSA) is used to analyze the temporal trends in CDHD indices (including $CDHD_f$, $CDHD_{ts}$, $CDHD_{as}$) and other climate outputs (including total precipitation, total PET, drought events, hot days and HDD) in maize growing seasons. MK trend test is based on the correlation between the ranks of a time series and their chronological order [76,77], which has the advantages of being rarely disturbed by outliers and easy to calculate. TSA, also known as Sen's slope estimator [78,79], provides a more robust slope estimate than the least-squares method because it is insensitive to outliers or extreme values. MK-TSA has been widely used to quantify the magnitude of trends in hydrometeorological time series. The Sen's slope of the trend can be calculated by:

$$\beta = \text{Median}\left(\frac{x_j - x_i}{j - i}\right) \quad (8)$$

where β is the slope of the trend, x_j and x_i ($i < j$) are time-series data of grid cells. $\beta > 0$ indicates that the time series shows an upward trend; $\beta < 0$ indicates that the time series shows a downward trend.

$$S = \sum_{i=1}^{n-1} \sum_{j=i+1}^n \text{sign}(x_j - x_i) \quad (9)$$

$$\theta = x_j - x_i \quad (10)$$

$$\text{sign}(\theta) = \begin{cases} 1 & \theta > 0 \\ 0 & \theta = 0 \\ -1 & \theta < 0 \end{cases} \quad (11)$$

$$E(S) = 0 \quad (12)$$

$$\text{Var}(S) = \frac{n(n+1)(2n+5)}{18} \quad (13)$$

$$Z = \begin{cases} \frac{S - 1}{\sqrt{\text{Var}(S)}} & S > 0 \\ 0 & S = 0 \\ \frac{S + 1}{\sqrt{\text{Var}(S)}} & S < 0 \end{cases} \quad (14)$$

where n is the number of data in time series. When the absolute value of Z is greater than 1.65, 1.96 and 2.58, the trend passes the significance test with reliability of 90%, 95% and 99% respectively.

2. Figures

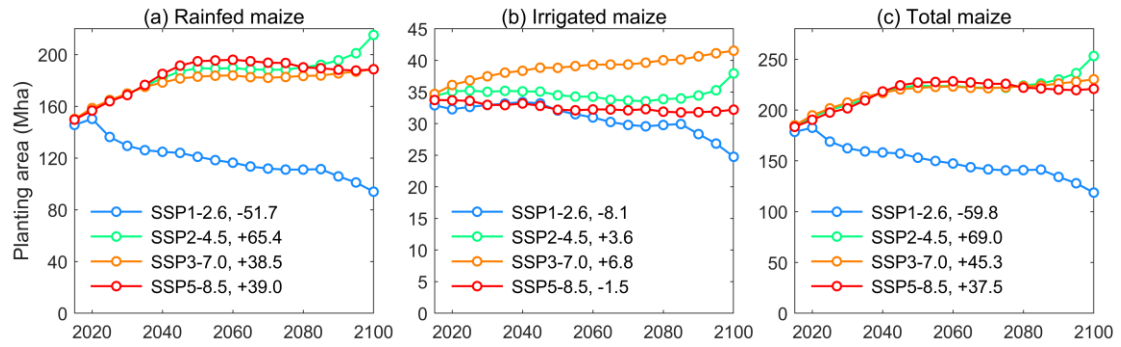


Figure S1. Changes in rainfed maize, irrigated maize and total maize planting areas over 2015-2100 under SSP1-2.6, SSP2-4.5, SSP3-7.0 and SSP5-8.5. Numbers are the difference in planting area between 2100 and 2015.

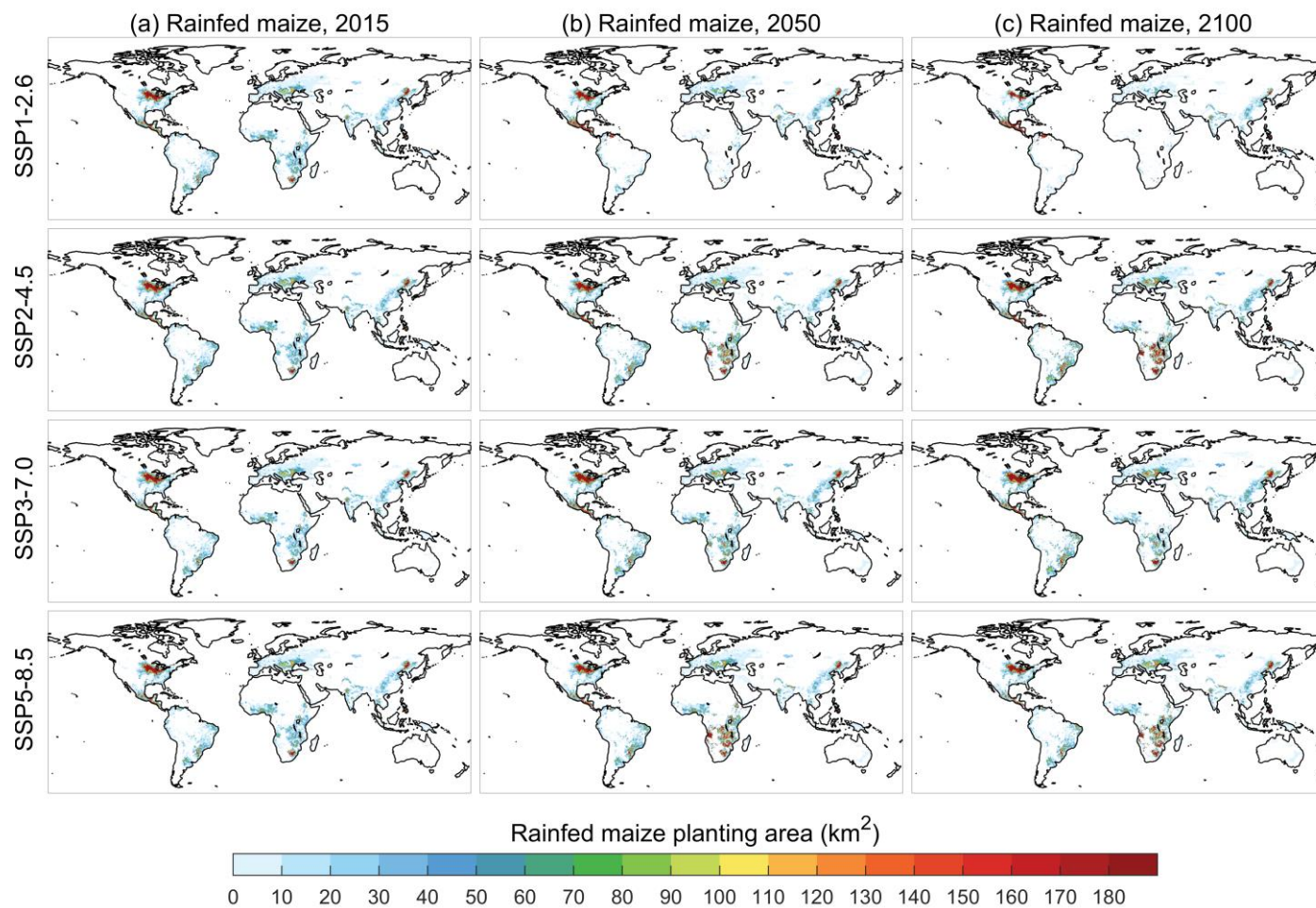


Figure S2. Global distribution of rainfed maize planting areas in 2015, 2050 and 2100 under SSP1-2.6, SSP2-4.5, SSP3-7.0 and SSP5-8.5.

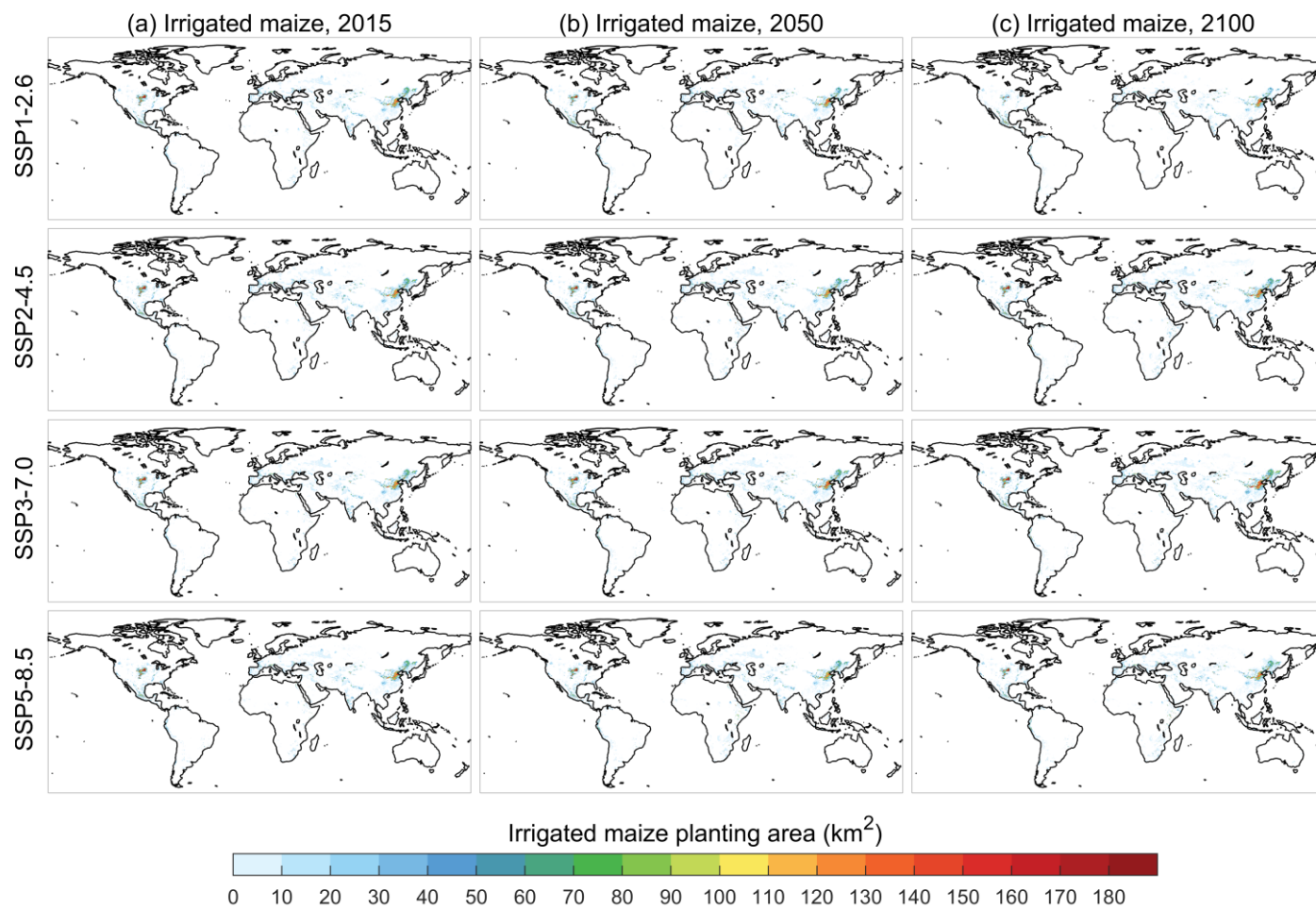


Figure S3. Global distribution of irrigated maize planting areas in 2015, 2050 and 2100 under SSP1-2.6, SSP2-4.5, SSP3-7.0 and SSP5-8.5.

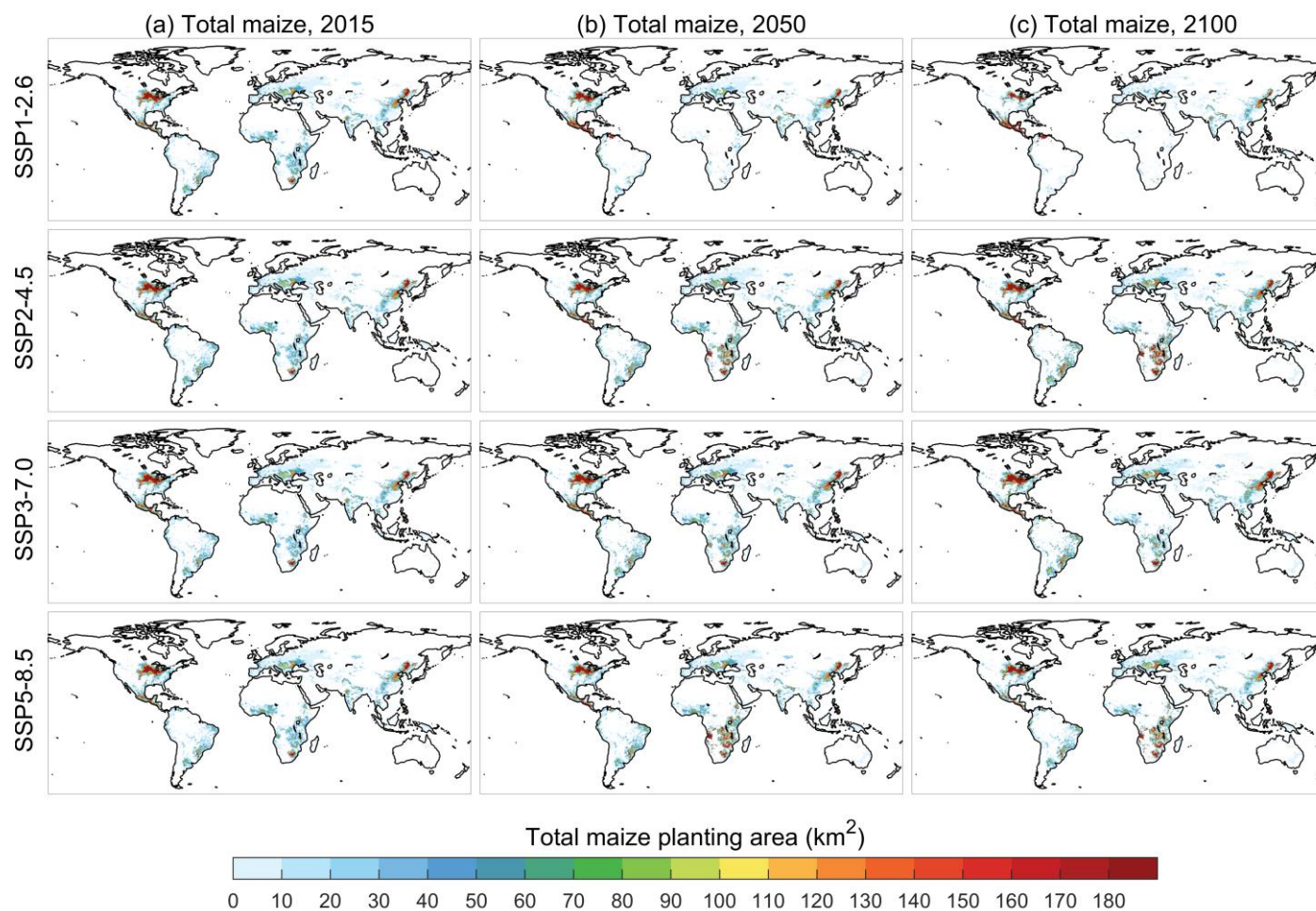


Figure S4. Global distribution of total maize planting areas in 2015, 2050 and 2100 under SSP1-2.6, SSP2-4.5, SSP3-7.0 and SSP5-8.5.

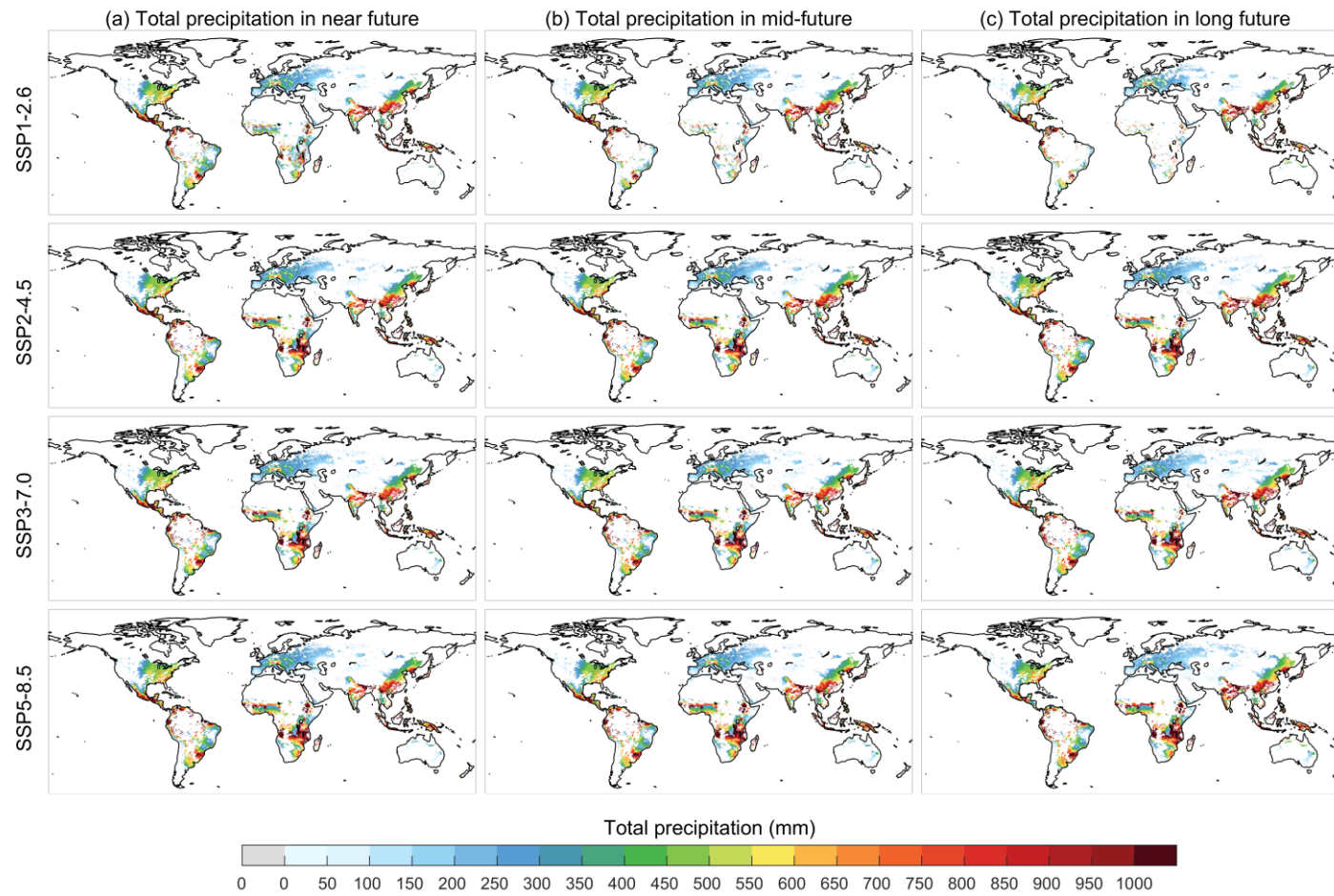


Figure S5. Global distribution of total precipitation in maize growing season in near future, mid-future and long future under SSP1-2.6, SSP2-4.5, SSP3-7.0 and SSP5-8.5.

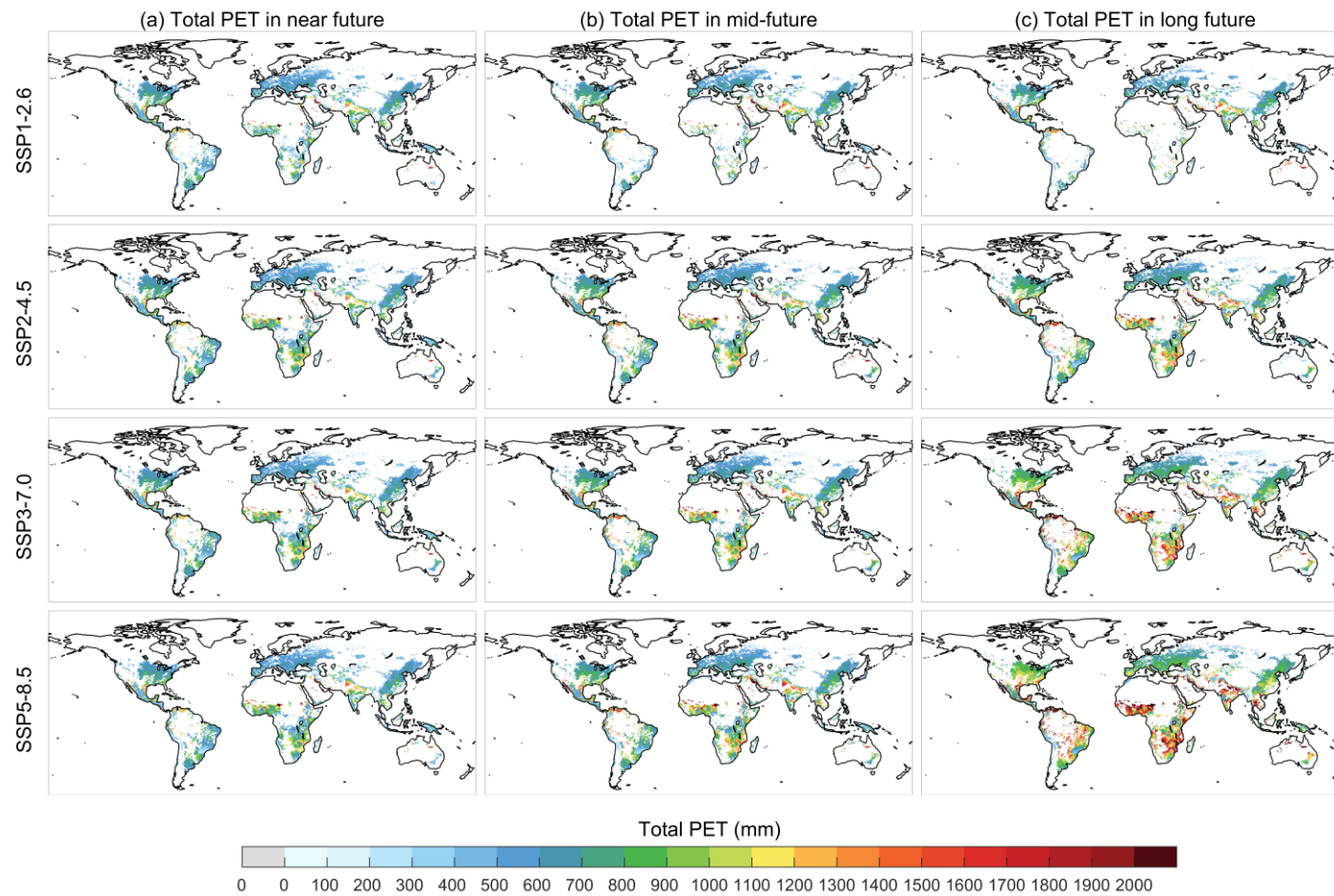


Figure S6. Global distribution of total PET in maize growing season in near future, mid-future and long future under SSP1-2.6, SSP2-4.5, SSP3-7.0 and SSP5-8.5.

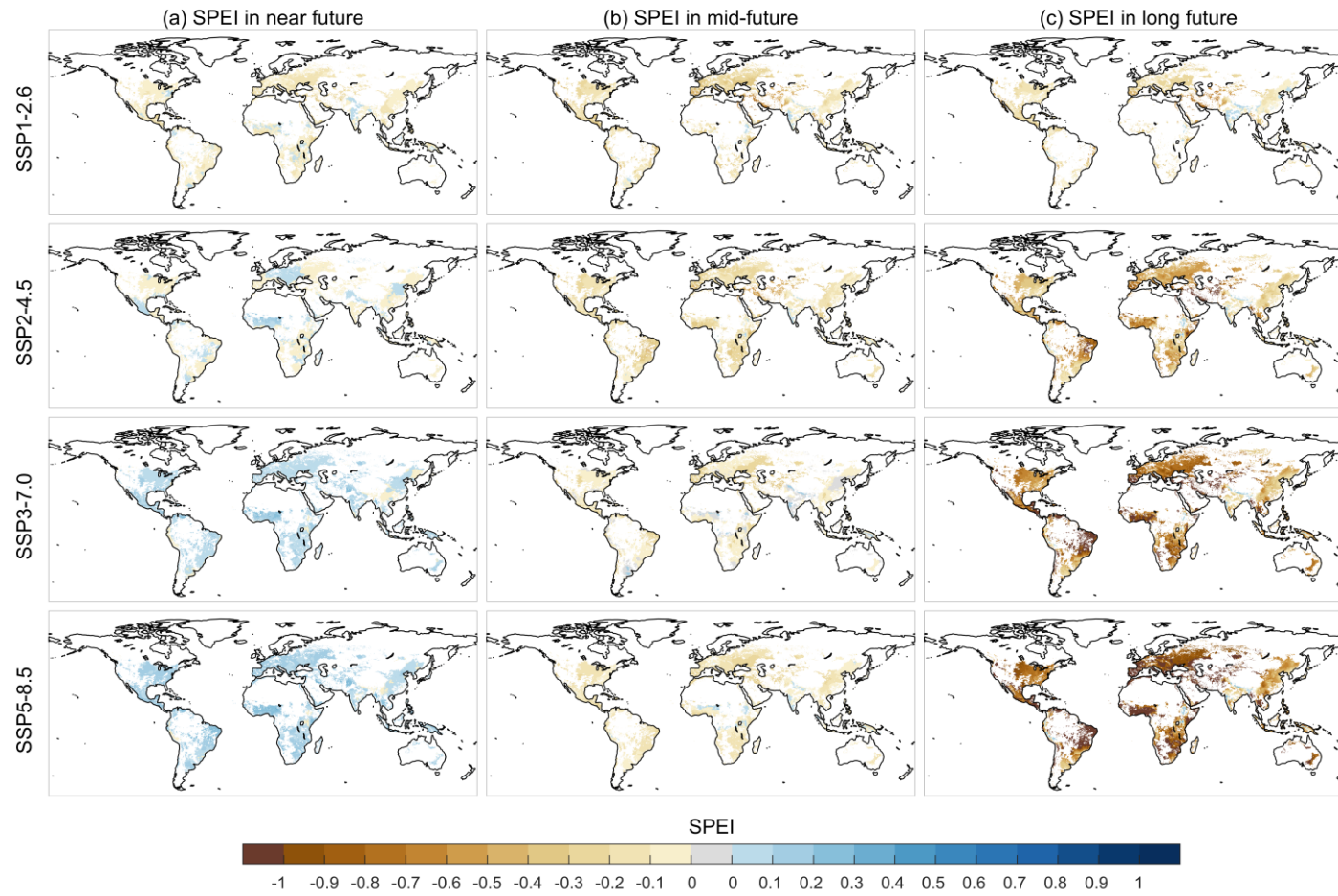


Figure S7. Global distribution of average SPEI in maize growing season in near future, mid-future and long future under SSP1-2.6, SSP2-4.5, SSP3-7.0 and SSP5-8.5.

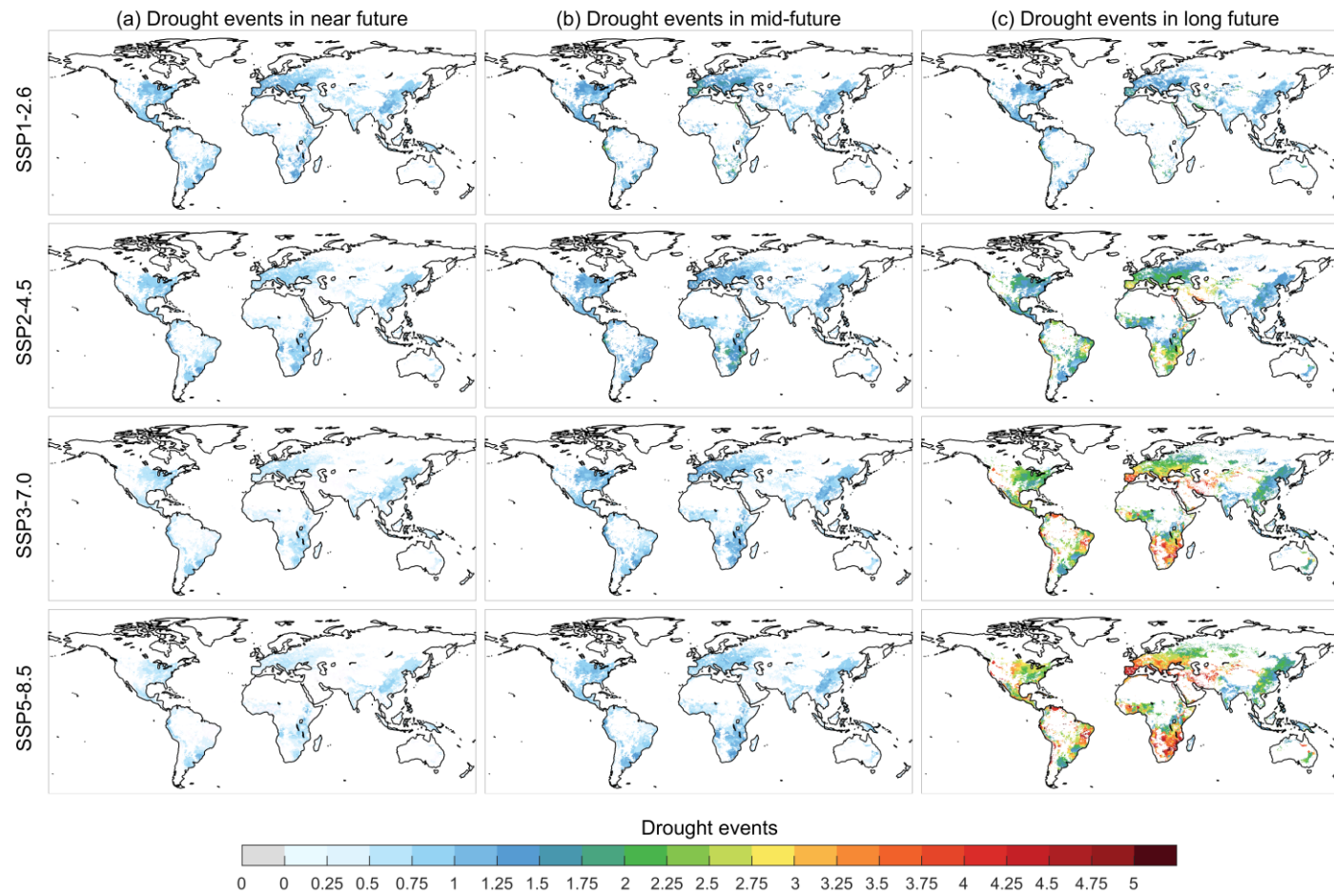


Figure S8. Global distribution of drought events in maize growing season in near future, mid-future and long future under SSP1-2.6, SSP2-4.5, SSP3-7.0 and SSP5-8.5.

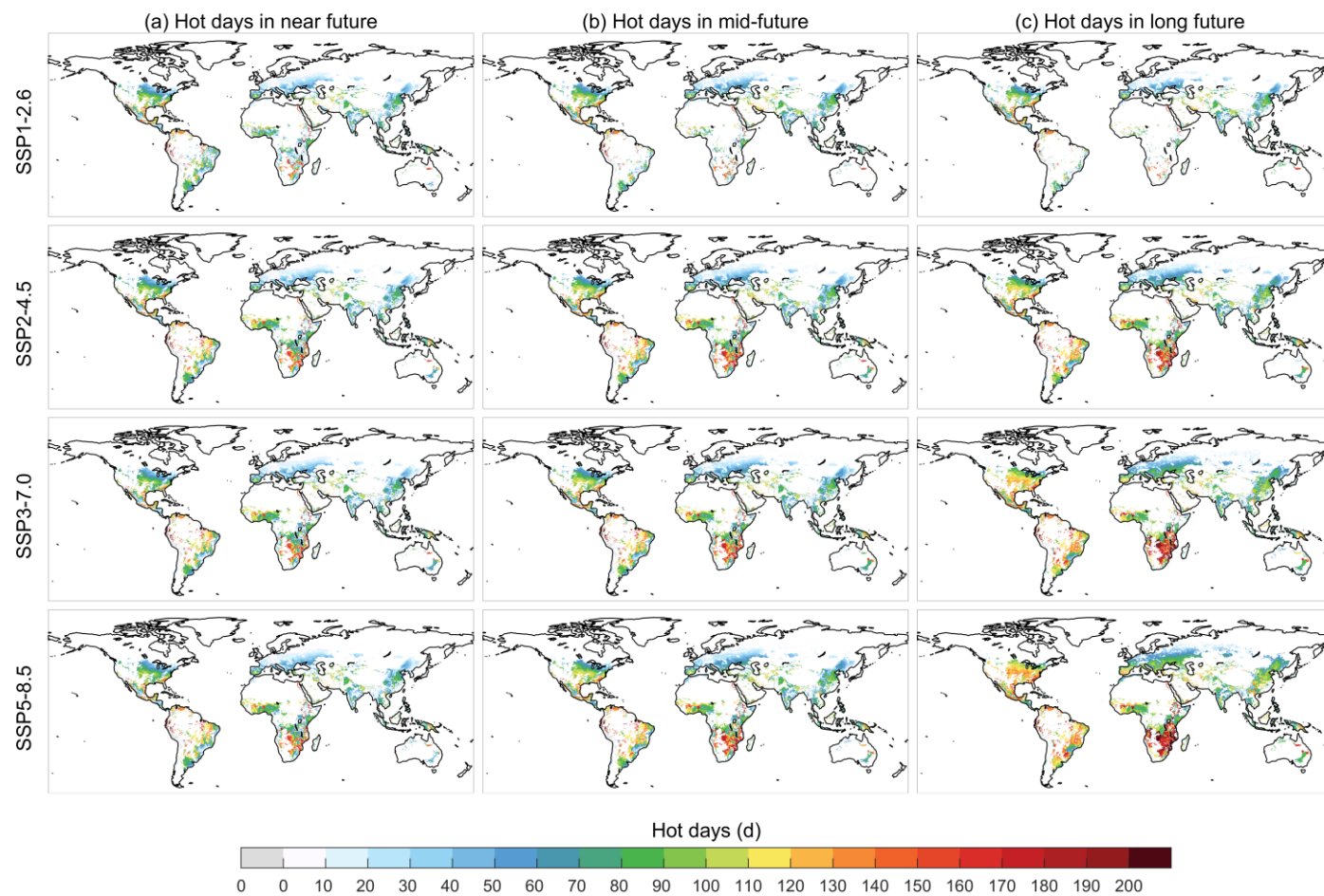


Figure S9. Global distribution of hot days in maize growing season in near future, mid-future and long future under SSP1-2.6, SSP2-4.5, SSP3-7.0 and SSP5-8.5.

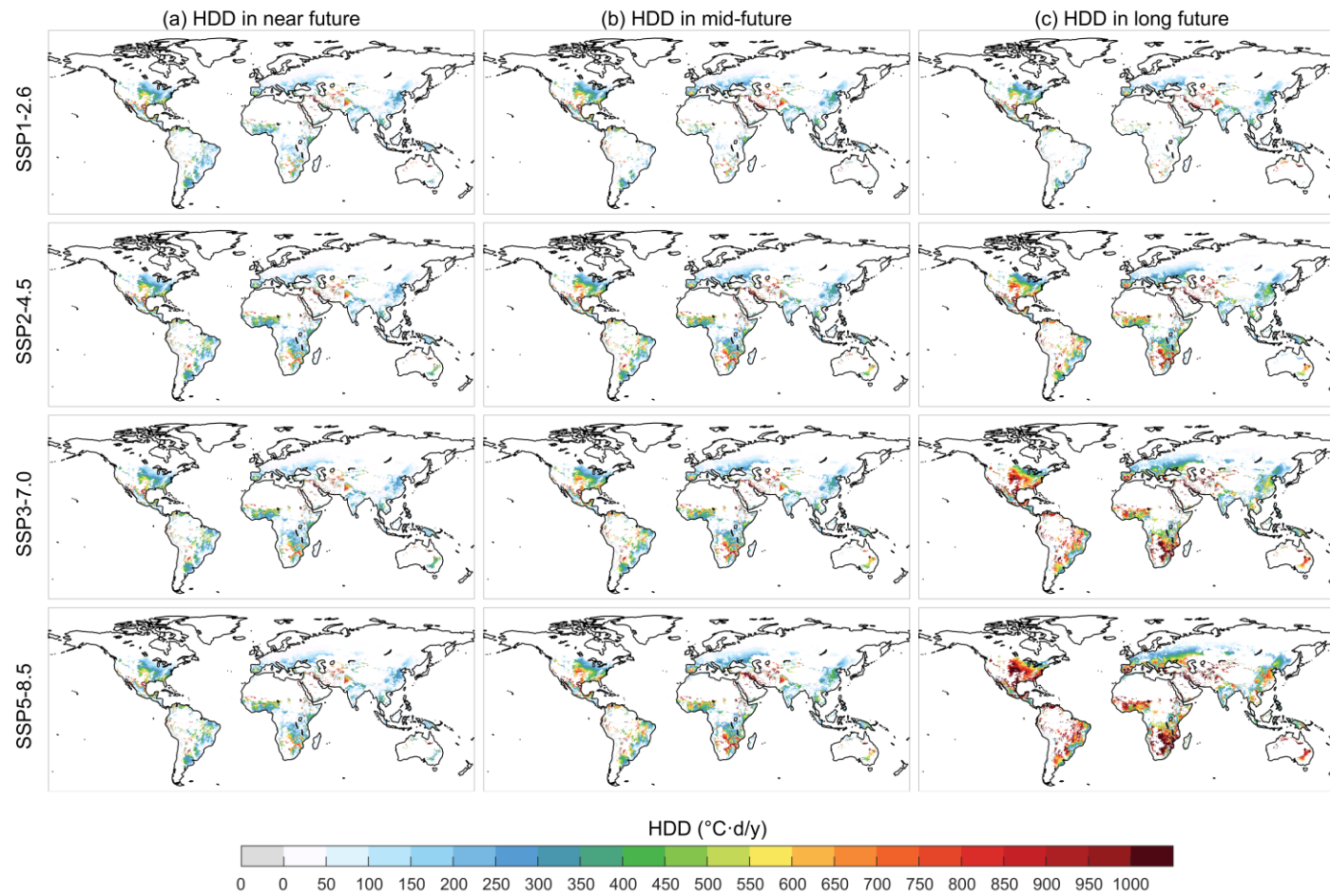


Figure S10. Global distribution of HDD in maize growing season in near future, mid-future and long future under SSP1-2.6, SSP2-4.5, SSP3-7.0 and SSP5-8.5.

3. Tables

Table S1. Regional maize import and export indicators (FAOStat, 2021).

Continent	Net imports (Mt)	Top importing (+) /exporting (-) countries (net import Mt)
Africa	16.2	
Eastern & Southern	-0.2	
Western & Central	0.9	
Northern	15.9	Egypt (+7.5)
Asia	69.2	
Southern	9.4	Iran (+ 7.9)
Eastern	34.2	Japan (+ 15.4); Republic of Korea (+ 10.3); China (+ 8.2)
Southeastern	13.8	Vietnam (+ 9.6)
Western & Central	11.8	
Americas	-80.2	
Northern	-53.7	United States (-53.8)
Central & Southern	-26.5	Brazil (-30.6); Argentina (-27.6); Mexico (+ 14.9); Colombia (+ 5.4); Paraguay (-2.1)
Europe	-9.9	Ukraine (-21.7); Spain (+ 8.9); Italy (+ 5.8); Romania (-4.5); Russia (-4.3); France (-3.6)
Oceania	0.1	

Table S2. GCMs from NEX-GDDP-CMIP6 used in this study.

Model name	Institution with country	Temporal resolution	Spatial resolution
ACCESS-CM2	CSRO-ARCCSS, Australia	Daily	$0.25^{\circ} \times 0.25^{\circ}$
CanESM5	CCCma, Canada		
CMCC-ESM2	CMCC, Italy		
EC-Earth3-Veg-LR	EC-Earth-Consortium, EU		
GFDL-ESM4	NOAA-GFDL, America		
INM-CM4-8	INM, Russia		
IPSL-CM6A-LR	IPSL, France		
MIROC6	MIROC, Japan		
MPI-ESM1-2-LR	MP1-M, Germany		
NorESM2-MM	NCC, Norway		